

4F Decreases IRF5 Expression and Activation in Hearts of Tight Skin Mice

Hao Xu¹, John G. Krolkowski², Deron W. Jones¹, Zhi-Dong Ge², Paul S. Pagel³, Kirkwood A. Pritchard, Jr.¹, Dorothee Weihrauch^{2*}

1 Division of Pediatric Surgery, Department of Surgery, Children's Research Institute, Milwaukee, Wisconsin, United States of America, **2** Division of Anesthesiology, Department of Surgery, Children's Research Institute, Milwaukee, Wisconsin, United States of America, **3** The Clement J. Zablocki Veterans Affairs Medical Center, Milwaukee, Wisconsin, United States of America

Abstract

The apoA1 mimetic 4F was designed to inhibit atherosclerosis by improving HDL. We reported that treating tight skin ($Tsk^{-/+}$) mice, a model of systemic sclerosis (SSc), with 4F decreases inflammation and restores angiogenic potential in $Tsk^{-/+}$ hearts. Interferon regulating factor 5 (IRF5) is important in autoimmunity and apoptosis in immune cells. However, no studies were performed investigating IRF5 in myocardium. We hypothesize that 4F differentially modulates IRF5 expression and activation in $Tsk^{-/+}$ hearts. Posterior wall thickness was significantly increased in $Tsk^{-/+}$ compared to C57Bl/6J (control) and $Tsk^{-/+}$ mice with 4F treatment assessed by echoradiography highlighting reduction of fibrosis in 4F treated $Tsk^{-/+}$ mice. IRF5 in heart lysates from control and $Tsk^{-/+}$ with and without 4F treatment (sc, 1 mg/kg/d, 6–8 weeks) was determined. Phosphoserine, ubiquitin, ubiquitin K^{63} on IRF5 were determined on immunoprecipitates of IRF5. Immunofluorescence and TUNEL assays in heart sections were used to determine positive nuclei for IRF5 and apoptosis, respectively. Fluorescence-labeled streptavidin (SA) was used to determine endothelial cell uptake of biotinylated 4F. SA-agarose pulldown and immunoblotting for IRF5 were used to determine 4F binding IRF5 in endothelial cell cytosolic fractions and to confirm bilayer interferometry studies. IRF5 levels in $Tsk^{-/+}$ hearts were similar to control. 4F treatments decrease IRF5 in $Tsk^{-/+}$ hearts and decrease phosphoserine and ubiquitin K^{63} but increase total ubiquitin on IRF5 in $Tsk^{-/+}$ compared with levels on IRF5 in control hearts. 4F binds IRF5 by mechanisms favoring association over dissociation strong enough to pull down IRF5 from a mixture of endothelial cell cytosolic proteins. IRF5 positive nuclei and apoptotic cells in $Tsk^{-/+}$ hearts were increased compared with controls. 4F treatments decreased both measurements in $Tsk^{-/+}$ hearts. IRF5 activation in $Tsk^{-/+}$ hearts is increased. 4F treatments decrease IRF5 expression and activation in $Tsk^{-/+}$ hearts by a mechanism related to 4F's ability to bind IRF5.

Citation: Xu H, Krolkowski JG, Jones DW, Ge Z-D, Pagel PS, et al. (2012) 4F Decreases IRF5 Expression and Activation in Hearts of Tight Skin Mice. PLoS ONE 7(12): e52046. doi:10.1371/journal.pone.0052046

Editor: Rajesh Gopalrao Katara, University of Otago, New Zealand

Received: September 7, 2012; **Accepted:** November 8, 2012; **Published:** December 14, 2012

Copyright: © 2012 Xu et al. This is an open-access article distributed under the terms of the Creative Commons Attribution License, which permits unrestricted use, distribution, and reproduction in any medium, provided the original author and source are credited.

Funding: Dorothee Weihrauch HL-089779, Kirkwood A. Pritchard Jr. HL-102836 and HL-102996, Hao Xu's start-up funds from Dept. Surgery, Div. Pediatric Surgery, and departmental funds from the Department of Anesthesiology. The funders had no role in study design, data collection and analysis, decision to publish, or preparation of the manuscript.

Competing Interests: The authors have declared that no competing interests exist.

* E-mail: dorothee@mcw.edu

Introduction

Scleroderma is an autoimmune disease that is characterized by marked increases in fibrosis of the skin and internal organs in conjunction with enhanced apoptosis [1]. The tight skin ($Tsk^{-/+}$) mouse is a murine model of systemic scleroderma that replicates many of the features observed in patients suffering from this disease [2]. Previously, we showed that $Tsk^{-/+}$ mice have impaired endothelial vasodilatation and angiogenic responses to VEGF that coincided with marked increases in angiotensin [3]. We also showed that the matrix isolated from the hearts of $Tsk^{-/+}$ mice stimulated endothelial cells (EC) to transition into fibroblasts and assume a more fibrotic phenotype [1]. Thus the extracellular matrix appears to play an important role in the mechanisms responsible for the vascular abnormalities in these mice. 4F is an apoA-I mimetic that was designed to improve high-density lipoprotein (HDL) function and has been shown to decrease proinflammatory HDL levels [4,5]. Our laboratory has observed that not only do 4F treatments inhibit vascular disease in $Tsk^{-/+}$

mice but even appear to delay the onset of heart failure in $Tsk^{-/+}$ mice (Figure 1).

Although there is much support for the idea that 4F inhibits atherosclerosis by improving HDL function [6], the mechanism by which 4F decreases inflammation has not been identified completely. Several mechanisms have been proposed including improvements in reverse cholesterol transport [7], formation of pre β HDL with improved HDL-dependent cholesterol efflux [4] and even greater affinity for oxidized rather than native lipids [8]. During the course of our studies for our report [1,3], we found the anti-inflammatory effects of 4F on the $Tsk^{-/+}$ mice to be so profound that it was difficult to attribute all of the effects solely to improvements in HDL function. While the published mechanisms may play important roles in the prevention of atherosclerosis none seemed sufficient for explaining why 4F protects vascular function and decreases inflammation in $Tsk^{-/+}$ mice, an extreme murine model of autoimmune disease. To better understand this paradox, we began to investigate alternative mechanisms for 4F protecting the myocardium in $Tsk^{-/+}$ mice.

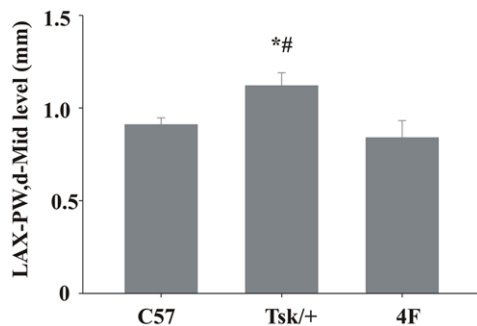


Figure 1. Echocardiography of hearts from Tsk/+ mice with and without 4F treatment and C57Bl/6J mice as control mouse. Posterior wall thickness was significantly improved by 4F treatment in the Tsk/+ mice ($p < 0.05$). doi:10.1371/journal.pone.0052046.g001

IRF5 is a transcription factor that has been called a “master switch” in immunity because it directs responses in macrophages and other inflammatory cells [9,10] and has been implicated as a key mediator of apoptosis [11,12]. Although much research has defined IRF5 cell biology in immune cells, little if any research is available concerning the role of IRF5 in the myocardium. In the current study we examine the effects of 4F on IRF5 in the hearts of Tsk^{-/+} mice and test the hypothesis that 4F decreases myocardial inflammation in the Tsk^{-/+} mice by inhibiting IRF5.

Materials and Methods

Peptide Synthesis

4F (Ac-DWFKAFYDKVAEKFKAEAF-NH₂) and biotin-labeled 4F (B-4F, biotin-labeled DWFKAFYDKVAEKFKAEAF-NH₂) were synthesized by Fmoc techniques using all D-amino acids (GenScript USA Inc, Piscataway, NJ). B-4F was synthesized in the same way but with one more cycle of synthesis with Fmoc-Lys(biotinyl-ε-aminocaproyl)-OH. Peptides were synthesized, purified by HPLC (>95%), and the purity confirmed by mass spectrometry by GenScript USA Inc [3].

Mice and Experimental Treatments

All experimental procedures and protocols involving mice were reviewed and approved by the Institutional Animal Care and Use Committee (IACUC) of the Medical College of Wisconsin (AUA#512). They also conformed to the rules in the *Guiding Principles in the Care and Use of Animals* published by the American Physiologic Society and the *Guide for the Care and Use of Laboratory Animals* published by OLAW. Male Tsk^{-/+} and C57Bl/6J mice (6–8 weeks of age) were purchased from Jackson Laboratories (Bar Harbor, ME). Three groups of mice were studied; C57Bl/6J, Tsk^{-/+}, and Tsk^{-/+} mice treated with 4F (1 mg/kg/d, sc) as published previously [3].

Transthoracic Echocardiography

Tsk^{-/+} and C57Bl/6J mice ($n = 6$) were anesthetized by isoflurane inhalation (1.50%) and oxygen. They were placed on a warming platform supine position. A VisualSonics Vevo 770 high-resolution imaging system (Toronto, Canada) equipped with a 30-MHz transducer (Scanhead RMV 707) was used to perform the transthoracic echocardiography. Two-dimensional guided M-mode LV dimensions were measured [13] and posterior wall thickness was analyzed.

IRF5 Expression

Hearts harvested from C57Bl/6J, Tsk^{-/+} and 4F-treated Tsk^{-/+} mice were snap-frozen and stored at -80°C for subsequent analysis. Frozen hearts were pulverized in a stainless steel mortar and pestle bathed in liquid nitrogen. The frozen powder was dissolved and homogenized in lysis buffer [MOPS pH 7.0, 20 mM; EGTA 2 mM; EDTA 5mM; NaF 30 mM; Protease Inhibitor Cocktail (Complete Mini Roche, Roche, Madison WI); Phosphatase Inhibitor Cocktail (Sigma P5726)]. Lysate proteins were quantified using BCA (bicinchoninic acid) reagent (Pierce, Rockford, IL). An aliquot of 40 μg lysate protein was diluted in Laemmli sample buffer [3,14] containing mercaptoethanol and heated to 95°C for 5 minutes, loaded onto SDS page gels (4–15%) and proteins separated by electrophoresis as described [1]. Proteins were transferred onto nitrocellulose membranes and blocked in Tris buffered saline (TBS) containing Tween (0.05%, TBS-T) and 10% non-fat dry milk for one hour and incubated with rabbit anti-IRF5 antibody (Protein-Tech, Chicago, IL; 1:800 dilution in TBS). The next day blots were washed two times, 5 minutes each time, in TBS-T and incubated with a HRP-conjugated anti-rabbit antibody (Santa Cruz Biotechnologies, Santa Cruz, CA, 1:5000 dilution) for one hour. Levels of IRF5 were obtained by scanning autoradiograms that were generated on Gene Mate film (BioExpress, Kayville, UT) with ECL plus Western Blotting Reagents (GE Healthcare, Piscataway, NJ) and developed with Kodak reagents (Rochester, NY). Images of band densities in the autoradiograms were captured using Photostudio software (ArcSoft, Fremont, CA) and a flatbed scanner (Canon, Model N12204 Lake Success, NY). Band densities were analyzed using Image J software (NIH, Bethesda, MD) [3].

IRF5 Post Translational Modifications

To determine the effects of strain and 4F treatments on the activation state of IRF5 we immunoprecipitated IRF5 from heart homogenates and examined changes in phosphoserine and ubiquitination on IRF5 using previously published protocols [14,15]. Briefly, heart homogenates were precleared with agarose beads for 1 hour followed by addition of anti-IRF5 antibody (Santa Cruz Biotechnologies) to the homogenates (500 μg in 0.5 ml) at 5 μg/100 μl (final concentration). Samples were incubated for 16 h at 4°C with end-over-end mixing. A 50 μl aliquot of a 50% slurry of Protein A agarose beads (Santa Cruz Biotechnologies) was added and incubated for 2 h with end-over-end mixing to pull-down immunocaptured IRF5. The beads were isolated by centrifugation and washed 3 times (3 minutes each time) in PBS. IRF5 was released from the beads with Laemmli sample buffer (Bio-Rad, Hercules, CA) containing mercaptoethanol and heating to 95°C for 5 min. IRF5 was separated from co-precipitated proteins by SDS-PAGE (4–15% Tris-HCl Criterion gels, Bio-Rad) and the proteins transferred onto nitrocellulose membranes. Membranes were blocked in 10% non-fat dry milk and then incubated in 2% non-fat dry milk containing polyclonal rabbit anti-phosphoserine (Antibodies-Online, Atlanta, GA, 1:200 dilution), monoclonal mouse anti-ubiquitin (Santa Cruz Biotechnologies, 1:200 dilution) or monoclonal mouse anti-K⁶³ ubiquitin (Enzo, Farmingdale, NY, 1:500 dilution) overnight at 4°C . The next day, the membranes were gently washed and incubated with the HRP-conjugated donkey anti-rabbit antibody (1:5,000, Santa Cruz Biotechnologies). Autoradiograms were developed; images of bands captured and densities analyzed as described above.

Measurements of IRF5 Positive Nuclei

Hearts were harvested from mice, flash frozen and imbedded in OCT and cut into 10 μm sections. Frozen sections were fixed for 10 minutes in PBS containing 1% paraformaldehyde. Cell membranes were permeabilized by incubation in PBS containing 0.5% Triton-X for 5 min at room temperature. The sections were washed once in PBS (5 min) and incubated in PBS containing mouse monoclonal anti-IRF5 antibody (Santa Cruz, 1:50 concentration) for 30 min at 37°C. Unbound anti-IRF5 antibody was washed free from the sections with PBS and the slides incubated with the appropriate Alexa 488-conjugated secondary antibody (Invitrogen, Carlsbad, CA) for 30 min at 37°C. The slides were washed two times with PBS and then incubated with TO-PRO 3TM for 3 min at room temperature (1 $\mu\text{g}/\text{ml}$, Invitrogen) to visualize cell nuclei. Sections were mounted in aqueous mounting media and analyzed by confocal microscopy [16,17].

Measurements of Apoptotic Cells

Hearts were harvested from mice, flash frozen and imbedded in OCT and cut into 10 μm sections. A TUNEL assay was performed on the sections using an ApopTag Plus Fluorescein labeled kit (Millipore, Billerica, MA, Cat# S7111) as per the manufacturer's instructions. Briefly, the free 3'OH DNA termini were labeled *in situ* with an anti-digoxigenin antibody conjugated to fluorescein. Nuclei were stained with TO-PRO 3TM for 3 minutes (1 $\mu\text{g}/\text{ml}$, Invitrogen). Slides were mounted and analyzed by confocal microscopy (Nikon Eclipse TE2000-U, EZ-C1-2 10 software, Nikon, Melville, NY). Images were captured using 488 nm excitation for fluorescein and 633 nm for nuclear labeling. Intensity was measured using Nikon Element imaging software (Nikon) [1].

Cellular Uptake of B-4F

Human umbilical vein endothelial cells (EC; Lonza, Walkersville, MD) were incubated in EGM complete media containing 4F or B-4F (10 and 50 $\mu\text{g}/\text{ml}$) for 4 hours. The EC cultures were washed with PBS, fixed in PBS containing 1% paraformaldehyde, and permeabilized with PBS containing 0.5% Triton-X. The permeabilized sections were incubated with fluorescein-conjugated streptavidin (1 $\mu\text{g}/\text{ml}$) for 30 minutes followed by 3 PBS washes. The fixed and fluorescently labeled slides were mounted in aqueous mounting media and sections inspected and analyzed by confocal microscopy [18].

IRF5 and 4F Interactions

Biolayer Interferometry (BLI): Protein-protein interactions were determined by BLI using an Octet Red 96TM interferometer (ForteBio, Inc, Menlo Park, CA). IRF5 was purchased (GenScript USA Inc) and labeled with biotin (cat no. 21329, Thermo Fisher Scientific, Rockford, IL) at a ratio of 1:1, which is optimal for binding and packaging target proteins onto SA biosensors (MR18-0009, ForteBio) for studying protein-protein interactions. Biotin-labeled IRF5 (B-IRF5) was loaded onto SA-biosensors in PBS for 15 minutes to ensure saturation. The B-IRF5-loaded SA biosensors were incubated in PBS containing 4F (20 $\mu\text{g}/\text{ml}$) for 10 minutes and association measured by following increases in wavelength interference. Next the loaded biosensors were incubated in PBS alone for 10 minutes to measure dissociation of 4F from B-IRF5 by following decreases in wavelength interference [19].

B-4F Pulldown Assays: To determine whether 4F interacts with IRF5 in the presence of cytosol proteins, we performed 4F pulldown assays on EC cytosolic fractions spiked with recombinant

IRF5. Briefly, cytosolic EC fractions were precleared with SA agarose beads (Cat#15942-050, Invitrogen) for 30 minutes at 4°C. IRF5 interactions were enhanced by adding recombinant IRF5 (2% wt/vol, GenScript USA Inc.) to the endothelial cytosolic fractions. 4F and B-4F were added to the cytosolic fractions and incubated for 3 hours at 4°C. SA agarose beads were added and the samples mixed end-over-end overnight at 4°C. The following day the SA agarose beads were isolated by centrifugation. The proteins associated with B-4F were released from the beads with Laemmli buffer and separated by SDS-PAGE (4–15%) as above. IRF5 levels in the pulldown samples were determined by autoradiography of immunoblots as above [20].

Statistical Analysis

Statistical analysis of data within and between groups was performed with analysis of variance (ANOVA) for repeated measures followed by Bonferroni's modification of Student's t-test. The null hypothesis was rejected when $P < 0.05$. All data are expressed as mean \pm standard error of the mean (SEM).

Results

Echocardiography

To measure an improvement of heart function we measured posterior wall thickness by echocardiography. Posterior wall thickness was significantly higher in the $\text{Tsk}^{-/+}$ mice compared to C57Bl/6J and $\text{Tsk}^{-/+}$ mice treated with 4F ($p < 0.05$) (Figure 1).

Myocardial IRF5 Expression

IRF5 expression in $\text{Tsk}^{-/+}$ hearts was essentially the same as in control hearts (Figure 1, lane 2 vs. lane 1). Interestingly, 4F treatments markedly decreased IRF5 expression in $\text{Tsk}^{-/+}$ hearts compared with the levels in hearts isolated from untreated $\text{Tsk}^{-/+}$ mice (Figure 2, lane 3 vs. lane 2). Image analysis of band densities indicate that 4F treatments reduced IRF5 in $\text{Tsk}^{-/+}$ hearts by 78%.

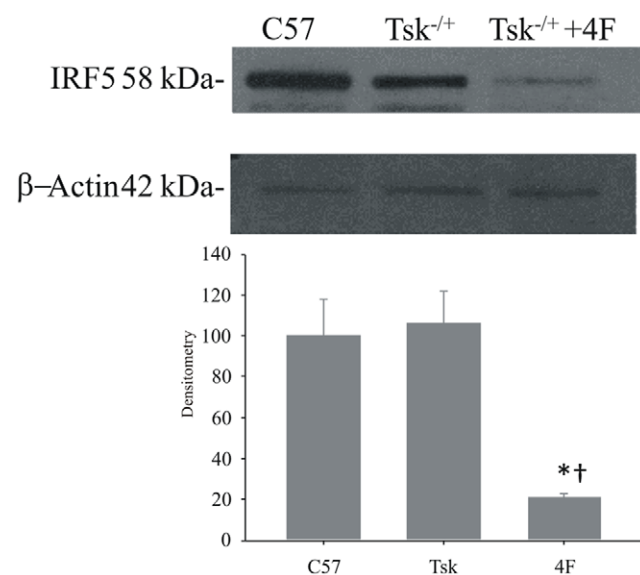


Figure 2. Western blot analysis of myocardial IRF5 protein expression. These blots show that IRF5 expression is unchanged in $\text{Tsk}^{-/+}$ myocardium when compared to C57Bl/6J myocardium. 4F treatments (s.c. 1 mg/kg/d for 6 weeks) however, markedly decrease IRF5 expression in $\text{Tsk}^{-/+}$ myocardium. doi:10.1371/journal.pone.0052046.g002

Myocardial IRF5 Phosphoserine and Ubiquitin

IRF5 activation is regulated by serine phosphorylation and ubiquitination [21,22]. Phosphoserine levels on IRF5 in $Tsk^{-/+}$ hearts were essentially the same as the levels on IRF5 in C57BL/6J hearts (Figure 3A). In contrast, the phosphoserine levels on IRF5 in 4F-treated $Tsk^{-/+}$ hearts were decreased by about 15% when compared with the levels on IRF5 in C57BL/6J and the untreated $Tsk^{-/+}$ hearts. Interestingly, total ubiquitin on IRF5 was increased in 4F-treated $Tsk^{-/+}$ hearts compared with the levels on IRF5 in C57BL/6J hearts (Figure 3B). The ubiquitinated lower band (Figure 3B, lane 3) may represent an inactive degradation product of IRF5 as the molecular weight of this band is notably less than the molecular weight of IRF5 in untreated $Tsk^{-/+}$ hearts (Figure 3B, lane 2). These post-translational changes in IRF5 coincided with marked decreases in IRF-5 nuclear localization (Figure 3) suggesting that the increase in ubiquitin on IRF5 in 4F-treated $Tsk^{-/+}$ mice may have resulted in IRF5 degradation rather than nuclear translocation. Although ubiquitination is reported to play a role in IRF5 translocation to the nucleus [23], ubiquitin K^{63} levels on IRF5 were actually decreased in hearts of $Tsk^{-/+}$ mice and increased in hearts of 4F-treated $Tsk^{-/+}$ mice (Figure 3C). These data suggest that IRF5 is activated in $Tsk^{-/+}$ hearts and inactivated in 4F-treated $Tsk^{-/+}$ hearts. Our observation that phosphoserine decreased and total ubiquitin increased on IRF5 in 4F-treated $Tsk^{-/+}$ hearts relative to the levels on IRF5 in untreated $Tsk^{-/+}$ hearts is consistent with this possibility. Taken together these changes suggest that 4F treatments inactivate IRF5 and increase its degradation in $Tsk^{-/+}$ hearts.

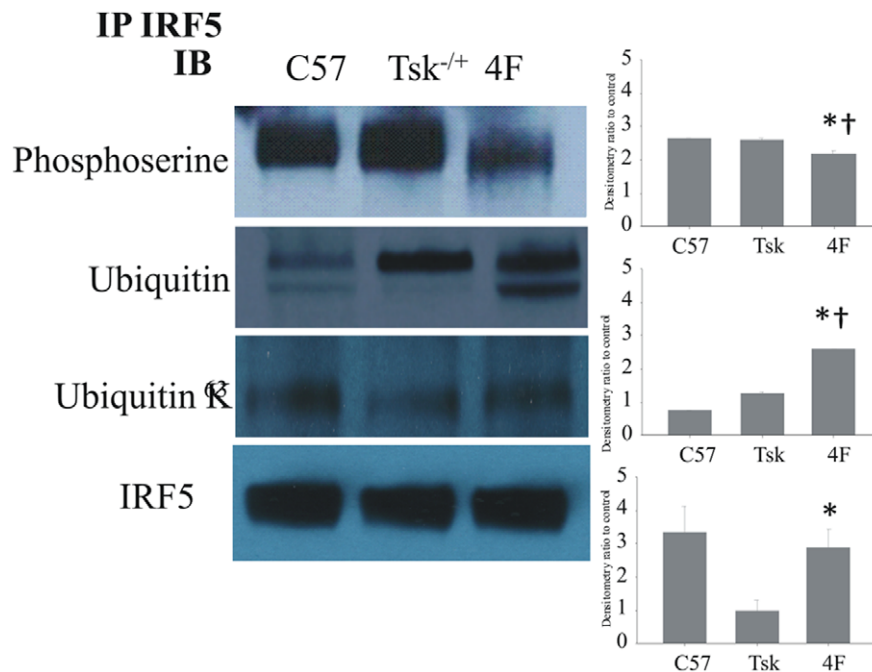


Figure 3. Western blot analysis of myocardial IRF5 immunoprecipitates. Western blot analysis of IRF5 immunoprecipitates from whole heart lysates shows that phosphoserine levels on IRF5 were essentially the same in $Tsk^{-/+}$ hearts as the levels on IRF5 in C57BL/6J hearts. 4F treatments reduced phosphoserine levels on IRF5 in $Tsk^{-/+}$ hearts compared with the levels on IRF5 in hearts from $Tsk^{-/+}$ and C57BL/6J mice. Total ubiquitin on IRF5 was upregulated in $Tsk^{-/+}$ hearts and 4F treatments of $Tsk^{-/+}$ mice, significantly increased total ubiquitin levels on IRF5 in the $Tsk^{-/+}$ hearts compared with the levels on IRF5 in C57BL/6J hearts (* = $p < 0.05$, $n = 4$). Finally, K^{63} ubiquitin on IRF5 in $Tsk^{-/+}$ hearts is decreased compared to the levels on IRF5 in C57BL/6J myocardium. 4F treatments of $Tsk^{-/+}$ mice increased K^{63} ubiquitin on IRF5 in $Tsk^{-/+}$ hearts with the levels on IRF5 from treated $Tsk^{-/+}$ mice being the highest when compared with levels in C57BL/6J and $Tsk^{-/+}$ myocardium.
doi:10.1371/journal.pone.0052046.g003

Myocardial IRF5 Positive Nuclei and Apoptotic Cells

Increased apoptosis is one of many hallmarks of scleroderma [24–26]. $Tsk^{-/+}$ hearts had more TUNEL positive cells than in C57BL/6J hearts (Figure 4). 4F treatments significantly decreased the number of TUNEL positive cells in $Tsk^{-/+}$ hearts compared to the number in untreated $Tsk^{-/+}$ hearts but not to the level of TUNEL positive cells in C57BL/6J hearts that actually had the least number of TUNEL positive cells (Figure 5).

Endothelial Cell Up-Take of 4F

If 4F modulates IRF5 activation then it likely enters the cells to do so. Confocal microscopy shows greater fluorescence in EC cultures incubated with 10 and 50 $\mu\text{g/ml}$ of B-4F than in EC cultures incubated with equal concentrations of unlabeled 4F (Figure 6). Image analysis of fluorescent intensity on a particle basis reveals that EC cultures incubated in media containing 50 $\mu\text{g/ml}$ of B-4F was significantly increased 3.6 fold ($p \leq 0.05$) compared with the intensities in EC cultures incubated with unlabeled 4F. EC cultures incubated in media containing B-4F at 10 $\mu\text{g/ml}$ concentration had an increase in fluorescence intensity that was approximately 30% more than the fluorescence in EC cultures in media containing unlabeled 4F.

4F-IRF5 Interactions

If 4F enters cells to modulate IRF5 expression and activation then it may also interact with IRF5. To determine if 4F interacts with IRF5 and to ascertain the nature of this interaction, we assessed rates of association and dissociation by biolayer interferometry. Our studies show that 4F rapidly associated with B-IRF5 bound to SA-biosensors. In contrast, dissociation of 4F from

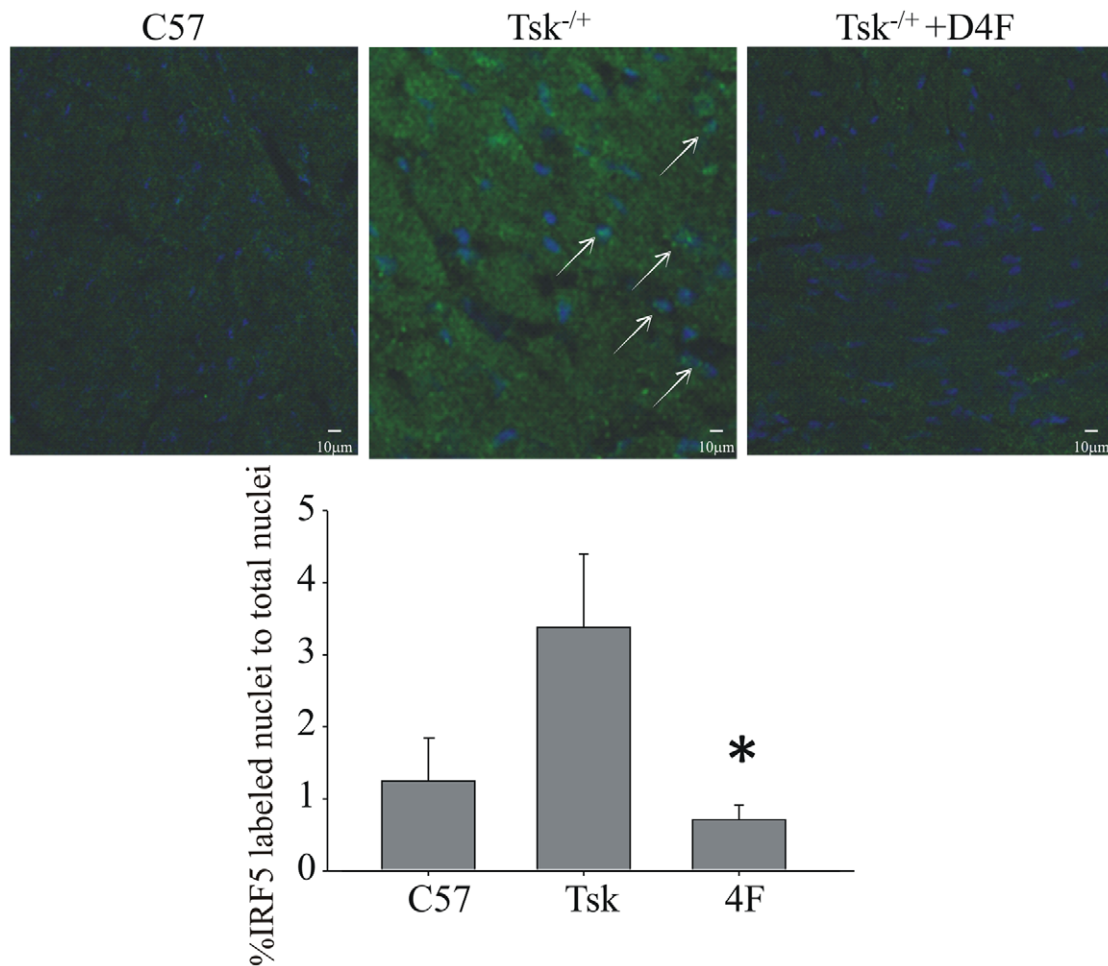


Figure 4. Immunohistochemistry for IRF5 depicted significantly more nuclear labeling in $Tsk^{-/-}$ hearts compared to C57BL/6J hearts and hearts from $Tsk^{-/-}$ mice treated with 4F. The bar graph shows the ratio between green IRF5 labeled nuclei to total nuclei number ($p < 0.05$, $n = 3$).

doi:10.1371/journal.pone.0052046.g004

B-IRF5 on SA biosensors was slow. These data suggest that the interaction of 4F with IRF5 favors association over dissociation (Figure 7). Simple pulldown assays confirm that B-4F associates with IRF5 even in the presence of EC cytosolic proteins (Figure 8).

Discussion

The purpose of this study was to investigate an alternative mechanism for 4F decreasing myocardial inflammation in $Tsk^{-/-}$ mice. While our previous report [3] focused on 4F's ability to decrease inflammation by improving HDL function, the current study determines the effects of 4F on IRF5. We chose to investigate this potential mechanism for two important reasons. First, others have already shown that 4F decreases expression of $TNF\alpha$, Il-6, and Il-1 [27,28]. These inflammatory mediators are all gene products of IRF5 [9,29]. Second, genetic links between IRF5 and SSc have been identified [30]. In this study we demonstrate that posterior wall thickness is significantly improved in $Tsk^{-/-}$ mice after 4F treatment highlighting the reduction of fibrosis in the $Tsk^{-/-}$ mice with 4F treatment even more. Together these reports provided the rationale for designing experiments to determine if 4F modulates IRF5 in the hearts of $Tsk^{-/-}$ mice. Data from the experiments show that while IRF5 levels in $Tsk^{-/-}$ hearts are comparable to their levels in control

hearts, IRF5 in $Tsk^{-/-}$ hearts is activated, present in myocardial cell nuclei and that hearts from untreated $Tsk^{-/-}$ have high levels of apoptotic cells. 4F treatments, on the other hand, decrease IRF5 expression, activation, nuclear translocation which begins to explain why hearts from 4F treated $Tsk^{-/-}$ mice are less inflamed and have fewer apoptotic cells than hearts from untreated $Tsk^{-/-}$ mice.

One of the reasons that we felt 4F decreased inflammation by a mechanism(s) other than those mediated by HDL function, was the extreme differences in the histopathology of the hearts from untreated and 4F treated $Tsk^{-/-}$ mice. Untreated $Tsk^{-/-}$ hearts contained much higher levels of oxidized phospholipids, and autoantibodies against oxidized lipids than control hearts [3]. In addition, untreated $Tsk^{-/-}$ hearts were also more fibrotic and expressed more angiostatin than control hearts, which likely contributed to the notable losses in angiogenic potential in the hearts of these mice [3]. When $Tsk^{-/-}$ mice were treated with 4F (1 mg/kg/d, 6–8 weeks), the treatment essentially eliminated oxidized phospholipids, and autoantibodies against oxidized phospholipids from the hearts. When the 4F-induced changes in myocardial inflammation in $Tsk^{-/-}$ mice were examined in light of other studies showing that 4F works better when HDL is present [7], we began to consider the notion that this small amphipathic

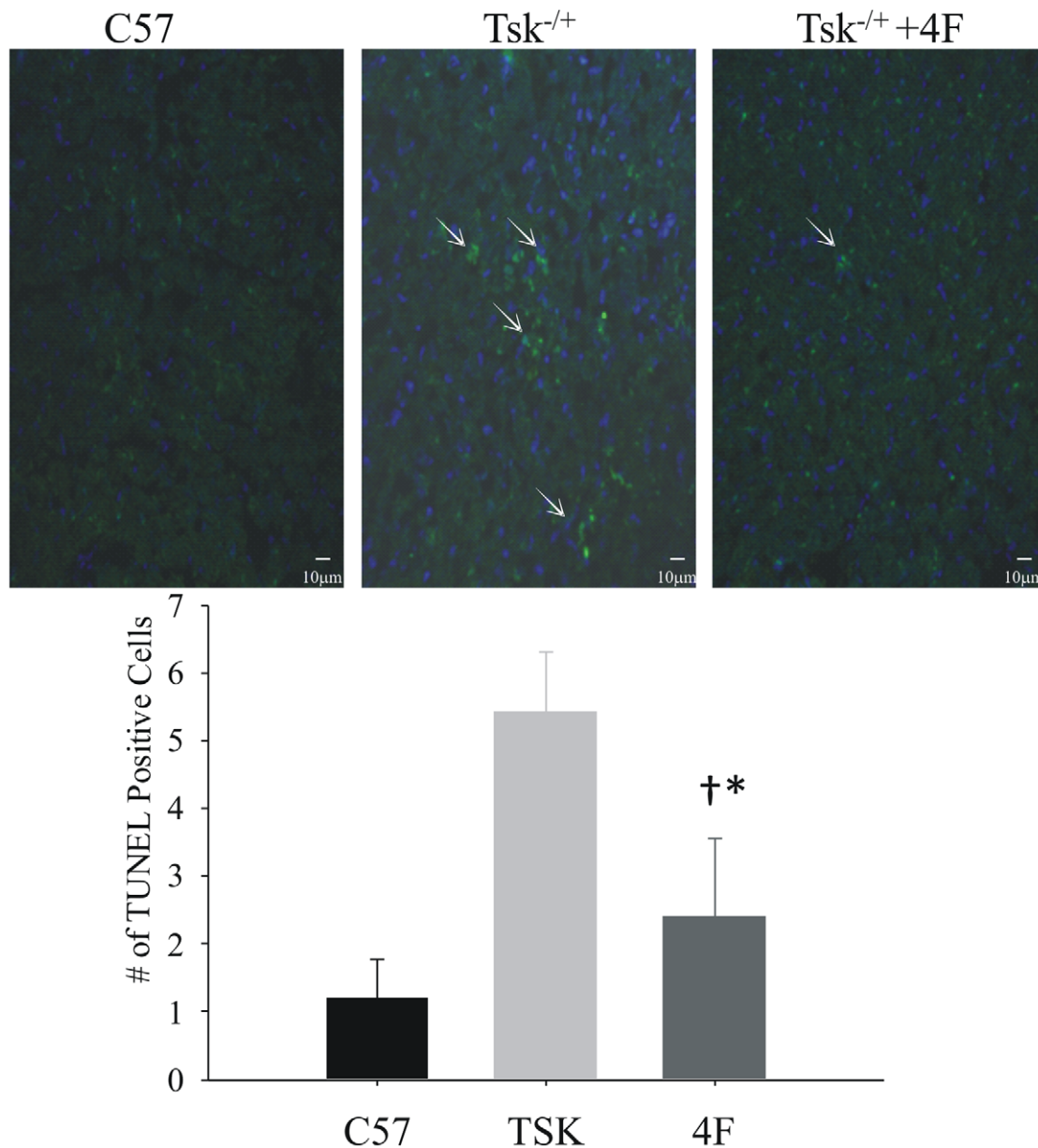


Figure 5. Apoptosis in the myocardium of C57BL/6J, $Tsk^{-/-}$ mice with and without 4F treatments. The number of apoptotic cells in C57BL/6J hearts is low. The number of apoptotic cells in the myocardium of $Tsk^{-/-}$ mice is increased compared with the levels in the hearts of C57BL/6J mice and hearts from 4F-treated $Tsk^{-/-}$ mice. doi:10.1371/journal.pone.0052046.g005

peptide inhibited mechanisms beyond those induced by proinflammatory HDL.

Although peptide mimetics and biologics have been used to target various mechanisms of disease, there is only one mimetic that we know of that specifically targets a transcription factor. COG₁₃₃ is reported to possess anti-inflammatory properties, not because it binds oxidized lipids but rather because it binds and inactivates NFkappaB. The efficacy of COG₁₃₃ was enhanced by linking the fragment to antennapedia to generate COG₁₁₂, thereby increasing its cellular uptake [31–33]. In addition, COG₁₁₂ inhibited NO production and iNOS expression in colonic epithelial cells [32]. Such observations lend support for the idea that small peptides may be useful tools for targeting transcription factors to inhibit oxidative stress.

In the current study, we showed that 4F enters EC in a concentration-dependent fashion even without a protein transduction domain. Our protein-protein interaction studies showed that 4F favors association over dissociation with IRF5 and that this interaction exists even in the presence of EC cytosolic proteins, where 4F must compete for access to IRF5. This observation however deserves an additional cautionary comment. We recognize that it is possible for 4F to interact with other cellular proteins, either in the membrane or in the signaling pathways mediating IRF5 expression and activation to indirectly down regulate IRF5. This possibility, and that 4F also has the potential to directly interact with IRF5 to decrease expression and activation will be investigated in much greater detail near future. Such studies are outside the scope of the current study.

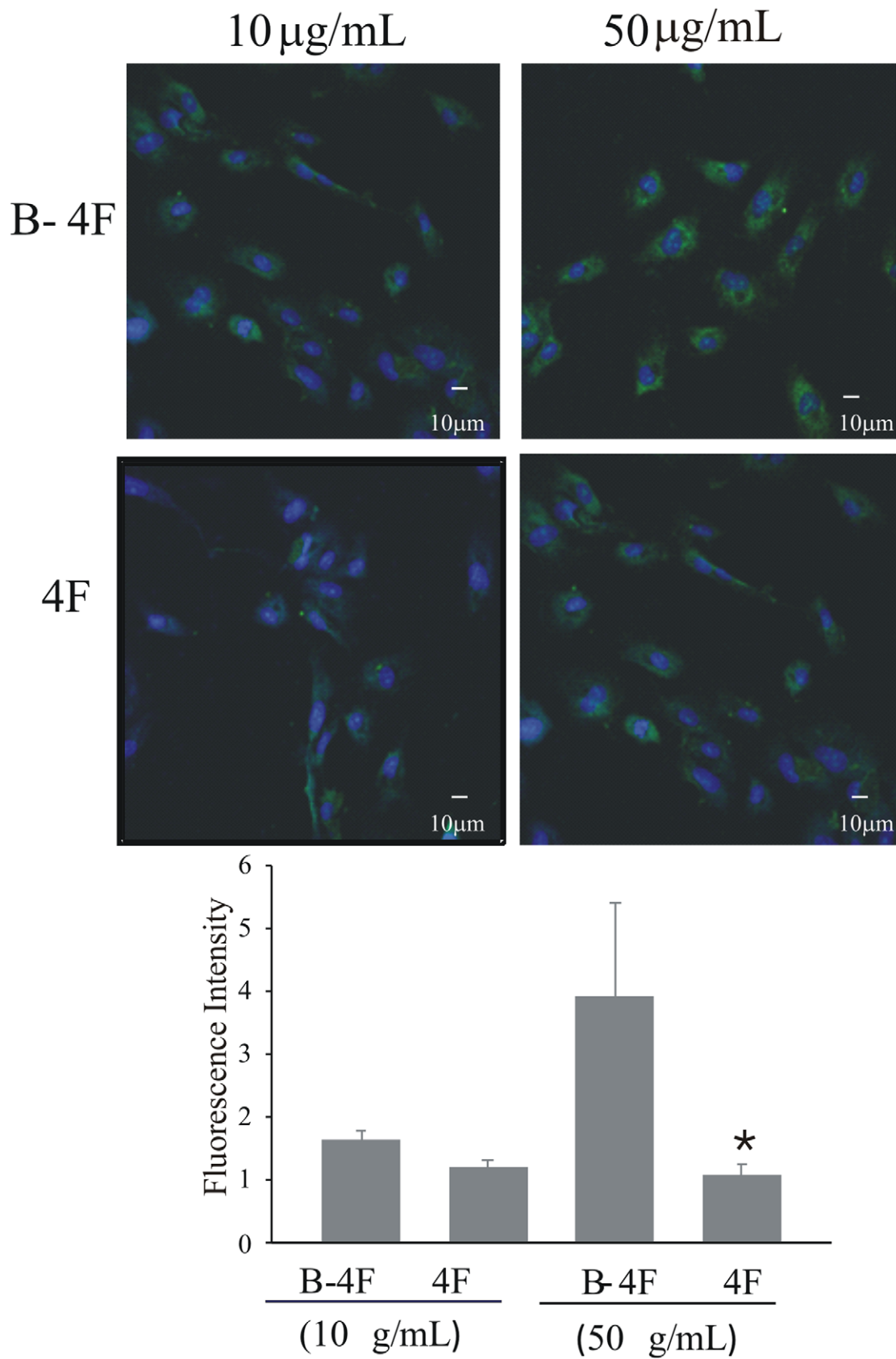


Figure 6. Cultured Endothelial Cells Take up 4F. EC cultures were treated with biotinylated 4F (B-4F) and unlabeled 4F. After 3 hours B-4F content is increased in ECs incubated with 10 and 50 µg/ml. doi:10.1371/journal.pone.0052046.g006

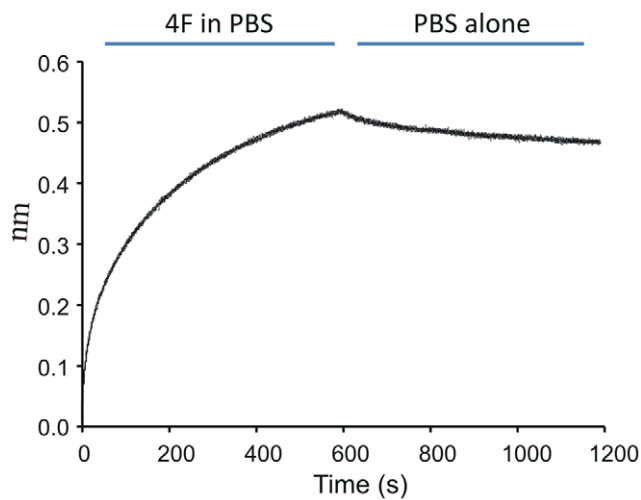


Figure 7. 4F interacts with IRF5. Interactions of 4F with IRF5 were determined by biolayer interferometry. These curves show that the rate of 4F association with IRF5 is faster than their rate of dissociation.
doi:10.1371/journal.pone.0052046.g007

Although there is overwhelming evidence in animal models that 4F improves HDL function and decreases atherosclerosis, our data are the first to suggest that 4F decreases inflammation by inhibiting IRF5 expression and activation. Therefore, our observations have important implications for future studies. First, they provide the rationale for designing agents that target IRF5 to protect against non-viral mediated inflammation of the heart. Second, IRF5 has the potential to preserve HDL function. Previous data showed a decrease of the atherogenic burden on HDL which might be associated with the inhibition of IRF5 [34]. Finally, as 4F appears to decrease myocardial inflammation by two distinct mechanisms they provide the rationale for developing agents that are specifically designed to distinguish between 4F's effects on classical mechanisms of atherogenesis and those mediated by IRF5.

Although much is known concerning the cell biology of IRF5 in immune cells, little, if any, information is available concerning the role of IRF5 in the myocardium. This is likely a result of the fact that monocytes, myeloid cells and B-lymphoblasts express IRF5 many fold higher than the levels of IRF5 in the heart [35]. Thus, a potential limitation in the current study is the possibility that the changes we observed in myocardial IRF5 expression may actually result from changes in immune cell content. However, it should be noted that preliminary histology studies revealed that cells with IRF5 positive nuclei were myocardial in nature rather than immune and that cultured neonatal myocytes surprisingly

References

- Xu H, Zaidi M, Struve J, Jones DW, Krolkowski JG, et al. (2011) Abnormal fibrillin-1 expression and chronic oxidative stress mediate endothelial mesenchymal transition in a murine model of systemic sclerosis. *American Journal of Physiology, Cell Physiology* 300: C550–6.
- Bocchieri MH, Henriksen PD, Jimenez SA, Kasturi KN, Muryoi T, et al. (1991) Evidence for autoimmunity in the tight skin mouse model of systemic sclerosis. *Arthritis & Rheumatism* 34: 599–605.
- Weihrauch D, Xu H, Shi Y, Wang J, Brien J, et al. (2007) Effects of D-4F on vasodilation, oxidative stress, angiotensin, myocardial inflammation, and angiogenic potential in tight-skin mice. *American Journal of Physiology, Heart and Circulatory Physiology* 293: H1432–41.
- Navab M, Anantharamaiah GM, Reddy ST, Hama S, Hough G, et al. (2004) Oral D-4F causes formation of pre-beta high-density lipoprotein and improves high-density lipoprotein-mediated cholesterol efflux and reverse cholesterol

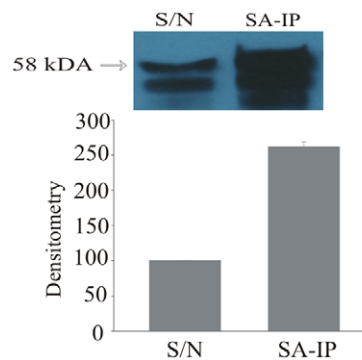


Figure 8. 4F Interacts with IRF5 in EC Lysates. This Western blot analysis of B-4F pull-down assays were performed on EC lysates to which recombinant IRF5 (10 μ g/mL, final concentration) was added. SA-agarose beads were used to pull down B-4F and associated proteins. In lane 2 is IRF5 bound to the B-4F precipitate is 2.5 fold higher than in control lane 1.
doi:10.1371/journal.pone.0052046.g008

expressed high levels of IRF5 that are also modulated by matrix in the same way as EC cultures [1,36].

Our results are the first to demonstrate that IRF5 is activated and present in the nuclei of cells in the myocardium of an established murine model of myocardial inflammation and fibrosis. Our findings are also the first to show that 4F decreases myocardial expression of IRF5, a transcription factor that others have shown is central to host-defense and inflammation in a variety of autoimmune diseases [30,36–38]. While our observations provide new insight into the anti-inflammatory properties of 4F, additional studies are required to determine how and why 4F alters the cell biology of IRF5 in *Tsk*^{-/+} mouse myocardium.

In conclusion, the current findings show that 4F decreases IRF5 levels and activation in the *Tsk*^{-/+} mouse hearts. Our observations demonstrate that 4F decreases myocardial inflammation by an alternative pathway in an established murine model of autoimmune disease. Our previous report and data here demonstrate that the mechanisms by which 4F decreases myocardial inflammation are multifactorial. Not only does 4F improve HDL function but it also targets IRF5 to decrease inflammation. Our results strongly suggest that developing specific inhibitors of IRF5 and/or their pathways of activation may result in new therapeutic modalities that would be capable of inhibiting inflammation and oxidative stress in autoimmune disease.

Author Contributions

Conceived and designed the experiments: HX PSP ZDG KAP DW. Performed the experiments: JK DJ DW KAP ZDG. Analyzed the data: HX JK ZDG KAP DW. Contributed reagents/materials/analysis tools: HX KAP DW. Wrote the paper: HX PSP KAP DW.

transport from macrophages in apolipoprotein E-null mice. *Circulation* 109: 3215–3220.

- Navab M, Anantharamaiah G, Reddy ST, Van Lenten BJ, Buga GM, et al. (2007) Peptide mimetics of apolipoproteins improve HDL function. *Journal of Clinical Lipidology* 1: 142–147.
- Charles-Schoeman C, Banquerigo ML, Hama S, Navab M, Park GS, et al. (2008) Treatment with an apolipoprotein A-1 mimetic peptide in combination with pravastatin inhibits collagen-induced arthritis. *Clinical Immunology* 127: 234–244.
- Navab M, Anantharamaiah G, Reddy ST, Van Lenten BJ, Ansell BJ, et al. (2004) Thematic review series: The pathogenesis of atherosclerosis the oxidation hypothesis of atherogenesis: The role of oxidized phospholipids and HDL. *Journal of Lipid Research* 45: 993–1007.

8. Van Lenten BJ, Wagner AC, Jung CL, Ruchala P, Waring AJ, et al. (2008) Anti-inflammatory apoA-I-mimetic peptides bind oxidized lipids with much higher affinity than human apoA-I. *Journal of Lipid Research* 49: 2302–2311.
9. Takaoka A, Yanai H, Kondo S, Duncan G, Negishi H, et al. (2005) Integral role of IRF-5 in the gene induction programme activated by toll-like receptors. *Nature* 434: 243–249.
10. Anda KS, Gómez-Martín D, Díaz-Zamudio M, Alcocer-Varela J (2011) Interferon regulatory factors: Beyond the antiviral response and their link to the development of autoimmune pathology. *Autoimmunity Reviews*.
11. Hu G, Barnes BJ (2009) IRF-5 is a mediator of the death receptor-induced apoptotic signaling pathway. *Journal of Biological Chemistry* 284: 2767–2777.
12. Couzinet A, Tamura K, Chen HM, Nishimura K, Wang Z, et al. (2008) A cell-type-specific requirement for IFN regulatory factor 5 (IRF5) in fas-induced apoptosis. *Proceedings of the National Academy of Sciences of the United States of America* 105: 2556–2561.
13. Nelson TJ, Ge ZD, Van Orman J, Barron M, Rudy-Reil D, et al. (2006) Improved cardiac function in infarcted mice after treatment with pluripotent embryonic stem cells. *The Anatomical Record. Part A, Discoveries in Molecular, Cellular, and Evolutionary Biology* 288: 1216–1224.
14. Amour J, Brzezinska AK, Weihrauch D, Billstrom AR, Zielonka J, et al. (2009) Role of heat shock protein 90 and endothelial nitric oxide synthase during early anesthetic and ischemic preconditioning. *Anesthesiology* 110: 317.
15. Weihrauch D, Lohr NL, Mraovic B, Ludwig LM, Chilian WM, et al. (2004) Chronic hyperglycemia attenuates coronary collateral development and impairs proliferative properties of myocardial interstitial fluid by production of angiotensin. *Circulation* 109: 2343–2348.
16. Oriyasa C, Kondo Y, Hayashi S, McEwen BS, Sakuma Y (2002) Sexually dimorphic expression of estrogen receptor β in the anteroventral periventricular nucleus of the rat preoptic area: Implication in luteinizing hormone surge. *Proceedings of the National Academy of Sciences* 99: 3306–3311.
17. Wilhelm JE, Buszczak M, Sayles S (2005) Efficient protein trafficking requires trailer hitch, a component of a ribonucleoprotein complex localized to the ER in *Drosophila*. *Developmental Cell* 9: 675–685.
18. Pardridge WM, Boado RJ (1991) Enhanced cellular uptake of biotinylated antisense oligonucleotide or peptide mediated by avidin, a cationic protein. *FEBS Letters* 288: 30–32.
19. Concepcion J, Witte K, Wartchow C, Choo S, Yao D, et al. (2009) Label-free detection of biomolecular interactions using biolayer interferometry for kinetic characterization. *Combinatorial Chemistry & High Throughput Screening* 12: 791–800.
20. Bruick RK, McKnight SL (2001) A conserved family of prolyl-4-hydroxylases that modify HIF. *Science Signalling* 24: 1337.
21. Kawai T, Akira S (2007) TLR signaling. *Immunity* 27: 24–32.
22. Balkhi MY, Fitzgerald KA, Pitha PM (2010) IKK α negatively regulates IRF-5 function in a MyD88–TRAF6 pathway. *Cellular Signalling* 22: 117–127.
23. Balkhi MY, Fitzgerald KA, Pitha PM (2008) Functional regulation of MyD88-activated interferon regulatory factor 5 by K63-linked polyubiquitination. *Molecular and Cellular Biology* 28: 7296–7308.
24. Ahmed SS, Tan FK, Arnett FC, Jin L, Geng YJ (2006) Induction of apoptosis and fibrillin 1 expression in human dermal endothelial cells by scleroderma sera containing anti-endothelial cell antibodies. *Arthritis & Rheumatism* 54: 2250–2262.
25. Hu G, Mancl ME, Barnes BJ (2005) Signaling through IFN regulatory factor-5 sensitizes p53-deficient tumors to DNA Damage–Induced apoptosis and cell death. *Cancer Research* 65: 7403.
26. Sgonc R, Gruschwitz MS, Dietrich H, Recheis H, Gershwin ME, et al. (1996) Endothelial cell apoptosis is a primary pathogenetic event underlying skin lesions in avian and human scleroderma. *Journal of Clinical Investigation* 98: 785.
27. Vecoli C, Cao J, Neglia D, Inoue K, Sodhi K, et al. (2011) Apolipoprotein A-I mimetic peptide L-4F prevents myocardial and coronary dysfunction in diabetic mice. *Journal of Cellular Biochemistry* 112: 2616–2626.
28. Handattu SP, Garber DW, Monroe CE, van Groen T, Kadish I, et al. (2009) Oral apolipoprotein A-I mimetic peptide improves cognitive function and reduces amyloid burden in a mouse model of alzheimer's disease. *Neurobiology of Disease* 34: 525–534.
29. Colonna M (2007) TLR pathways and IFN-regulatory factors: To each its own. *European Journal of Immunology* 37: 306–309.
30. Sharif R, Mayes MD, Tan FK, Gorlova OY, Hummers LK, et al. (2012) IRF5 polymorphism predicts prognosis in patients with systemic sclerosis. *Annals of the Rheumatic Diseases*.
31. Wool GD, Vaisar T, Reardon CA, Getz GS (2009) An apoA-I mimetic peptide containing a proline residue has greater in vivo HDL binding and anti-inflammatory ability than the 4F peptide. *Journal of Lipid Research* 50: 1889–1900.
32. Singh K, Chaturvedi R, Barry DP, Coburn LA, Asim M, et al. (2011) The apolipoprotein E-mimetic peptide COG112 inhibits NF-kappaB signaling, proinflammatory cytokine expression, and disease activity in murine models of colitis. *The Journal of Biological Chemistry* 286: 3839–3850.
33. Singh K, Chaturvedi R, Asim M, Barry DP, Lewis ND, et al. (2008) The apolipoprotein E-mimetic peptide COG112 inhibits the inflammatory response to citrobacter rodentium in colonic epithelial cells by preventing NF-kappaB activation. *The Journal of Biological Chemistry* 283: 16752–16761.
34. Ou J, Ou Z, Jones DW, Holzhauer S, Hatoum OA, et al. (2003) L-4F, an apolipoprotein A-I mimetic, dramatically improves vasodilation in hypercholesterolemia and sickle cell disease. *Circulation* 107: 2337–2341.
35. Su AI, Wiltshire T, Batalov S, Lapp H, Ching KA, et al. (2004) A gene atlas of the mouse and human protein-encoding transcriptomes. *Proceedings of the National Academy of Sciences of the United States of America* 101: 6062.
36. Krolkowski J, Jones D, Pritchard JK, Weihrauch D (2012) D-4F decreases myocardial inflammation in a model of murine scleroderma by decreasing interferon regulating factor-5 levels. *Atherosclerosis, Thrombosis, Vascular Biology* 32.
37. Kozyrev SV, Alarcon-Riquelme ME (2007) The genetics and biology of Irf5-mediated signaling in lupus. *Autoimmunity* 40: 591–601.
38. Graham RR, Kozyrev SV, Baechler EC, Reddy MVPL, Plenge RM, et al. (2006) A common haplotype of interferon regulatory factor 5 (IRF5) regulates splicing and expression and is associated with increased risk of systemic lupus erythematosus. *Nature Genetics* 38: 550–555.